materials

MDPI

Article

Mechanical Properties and Corrosion Behavior of Ti6Al4V Particles Obtained by Implantoplasty: An In Vitro Study. Part II

Jorge Toledano-Serrabona [1], Maria Ángeles Sánchez-Garcés [1,*], Cosme Gay-Escoda [1], Eduard Valmaseda-Castellón [1], Octavi Camps-Font [1], Pablo Verdeguer [2], Meritxell Molmeneu [3] and Francisco Javier Gil [2,4,*]

1 Bellvitge Biomedical Research Institute (IDIBELL), Department of Oral Surgery and Implantology, Faculty of Medicine and Health Sciences, University of Barcelona, 08907 Barcelona, Spain; jorgetoledano25@gmail.com (J.T.-S.); cgay@ub.edu (C.G.-E.); eduardvalmaseda@ub.edu (E.V.-C.); ocamps@ub.edu (O.C.-F.)
2 Bioengineering Institute of Technology, International University of Catalonia, 08195 Barcelona, Spain; pverdeguerm@gmail.com
3 Biomaterials, Biomechanics and Tissue Engineering Group (BBT), Department of Materials Science and Engineering, Polytechnic University of Catalonia, 08019 Barcelona, Spain; meritxell.molmeneu@upc.edu
4 Faculty of Dentistry, International University of Catalonia, 08195 Barcelona, Spain
* Correspondence: masanchezg@ub.edu (M.Á.S.-G.); xavier.gil@uic.es (F.J.G.)

Abstract: In the field of implant dentistry there are several mechanisms by which metal particles can be released into the peri-implant tissues, such as implant insertion, corrosion, wear, or surface decontamination techniques. The aim of this study was to evaluate the corrosion behavior of Ti6Al4V particles released during implantoplasty of dental implants treated due to periimplantitis. A standardized protocol was used to obtain metal particles produced during polishing the surface of Ti6Al4V dental implants. Physicochemical and biological characterization of the particles were described in Part I, while the mechanical properties and corrosion behavior have been studied in this study. Mechanical properties were determined by means of nanoindentation and X-ray diffraction. Corrosion resistance was evaluated by electrochemical testing in an artificial saliva medium. Corrosion parameters such as critical current density (icr), corrosion potential (E_{CORR}), and passive current density (i_{CORR}) have been determined. The samples for electrochemical behavior were discs of Ti6Al4V as-received and discs with the same mechanical properties and internal stresses than the particles from implantoplasty. The discs were cold-worked at 12.5% in order to achieve the same properties (hardness, strength, plastic strain, and residual stresses). The implantoplasty particles showed a higher hardness, strength, elastic modulus, and lower strain to fracture and a compressive residual stress. Resistance to corrosion of the implantoplasty particles decreased, and surface pitting was observed. This fact is due to the increase of the residual stress on the surfaces which favor the electrochemical reactions. The values of corrosion potential can be achieved in normal conditions and produce corroded debris which could be cytotoxic and cause tattooing in the soft tissues.

Keywords: implantoplasty; corrosion; Ti6Al4V; dental implant

Citation: Toledano-Serrabona, J.; Sánchez-Garcés, M.Á.; Gay-Escoda, C.; Valmaseda-Castellón, E.; Camps-Font, O.; Verdeguer, P.; Molmeneu, M.; Gil, F.J. Mechanical Properties and Corrosion Behavior of Ti6Al4V Particles Obtained by Implantoplasty: An In Vitro Study. Part II. *Materials* **2021**, *14*, 6519. https://doi.org/10.3390/ma14216519

Academic Editor: Alessandro Vichi

Received: 13 September 2021
Accepted: 25 October 2021
Published: 29 October 2021

1. Introduction

Commercially pure titanium (cp-Ti) dental implants are an excellent long-term treatment for patients with loss of teeth [1,2]. Titanium dental implants (grades I–IV) are highly reliable due to their excellent biocompatibility, mechanical characteristics, and good corrosion resistance among other properties [3–5]. However, the strongest grade of cp-Ti has a strength of around 550 MPa. Thus, other Ti alloys have been designed in order to increase the strength of the material [6]. Among Ti alloys, Ti6Al4V is an (α-β)-type that has been used in a wide range of biomedical purposes. This alloy was first developed in

the aerospace industry but due to its strength, excellent corrosion resistance, and biocompatibility, Ti6Al4V is used for biomedical purposes. There are some concerns related to the long-term use of Ti6Al4V that have already been outlined in Part I. In summary, as Ti6Al4V contains toxic V, different alloys such as Ti6Al7Nb, Ti5Al2.5Fe, or TiZr have been proposed to replace it. However, Ti6Al4V remains the most widely used Ti alloy for dental implants [6–11].

During the lifespan of dental implants, different complications may occur, such as mechanical, biological, and esthetic complications. Biological complications comprise peri-implant mucositis and peri-implantitis, both of which are inflammatory conditions induced by bacterial plaque affecting the surrounding tissues of the dental implant [12]. Nonsurgical treatment is sufficient for remission of peri-implant mucositis, but not for peri-implantitis. Depending on the type of peri-implant defect and the location of the implant, surgical treatment of peri-implantitis includes access surgery, resective surgery, peri-implant bone reconstruction (regenerative or reconstructive surgery), or a combination of these techniques [13]. Additionally, it is crucial to decontaminate the dental implant surface during nonsurgical or surgical procedures to stop the progression of the disease [14].

Metal particles of different sizes are generated during the insertion of the dental implant, bed preparation, machining to improve the fit of the prothesis, or wear due to micro-movements or functional loading. Dental implant surface decontamination procedures to treat peri-implantitis can also generate metallic debris. These particles with high internal energy can have significant physiological effects, such as an increase of the corrosion rate with generation of debris, cytotoxicity, an increase of ion release, and loss of the mechanical properties (such as crack nucleation on the surface resulting in fatigue). These aspects might disrupt osseointegration and cause bone resorption (osteolysis), which in turn may lead to implant loss [15–19].

The oral medium, with the presence of saliva, bacteria, other metals and alloys, and chemical products (for instance, gastric acids caused by reflux) causes corrosion and chemical degradation of titanium or titanium alloys [20–24].

In addition to the negative impact on biology, the corrosion of dental alloys can also have a negative effect on function and aesthetics of a dental prosthesis. The process of corrosion generates corrosion debris, which contains toxic oxides and metal ions that may not only come into contact with the surrounding cells and tissues, but also be distributed throughout the body through the bloodstream, intestines, and urinary excretory system. Debris particles of 10 to 20 μm in size have been detected at the implant surface and peri-implant bone, and distant sites, such as the lungs, liver, and kidney [25].

The purpose of this investigation was to describe the mechanical characteristics, including hardness and elastic modulus, as well as to determine the corrosion behavior of metal particles originating from commonly used Ti6Al4V (grade 5) following an implantoplasty procedure. This aims to raise the awareness of potential detrimental effects of implantoplasty and the need for careful consideration of the dental implant material.

2. Materials and Methods

2.1. Sample Preparation

A single investigator (J.T-S.) carried out implantoplasty procedures of Ti6Al4V dental implants following the drilling protocol described in previous publications [26,27]. A GENTLEsilence LUX 8000B turbine was used (KaVo Dental GmbH, Biberach, Germany) with water irrigation at room temperature. The surface was sequentially modified with a fine-grained tungsten carbide bur and two polishers, as described in Part I. The sample was lyophilized to rid the water from the metal particles.

2.2. Scanning Electron Microscopy and Mechanical Properties

As previously described in Part I, the morphometry of the sample was determined by scanning electron microscopy Neon 40 Surface Scanning Electron Focused Ion Beam Zeiss (Zeiss, Oberkochen, Germany).

A hardness analysis was performed using nanoindentation techniques on the dental implant (base material) and on the metal debris released during implantoplasty in order to determine the hardness and elastic modulus of both types of samples.

The nanoindentation assays were carried out using "Berkovich" type indenters, with a constant strain rate of 0.05 s^{-1}. An iMiro (KLA tencor, Kavo dental, Bibereach, Germany) and a Nanoindenter XP (MTS Systems Corporation, Oak Ridge, TN, USA) were used for the determination of implant hardness and metal debris hardness, respectively.

Residual stresses were measured with a diffractometer incorporating a Bragg–Brentano configuration (D500, Siemens, Wurzburg, Germany). Following Bragg's law, the superficial stress can be calculated since X-Ray diffraction allows the determination of the interplanar distance before and after shot blasting. After the treatment, the interplanar distance is smaller due to the residual compressive stress. The differences in the interatomic distance allow calculation of the microstrain, which, together with the elastic modulus of the material, allows the determination of the residual stress on the surface. The measurements were done for the family of planes (213) which diffracts at $2\theta = 139.5°$. The elastic constants of Ti at the direction of this family of planes are $EC = (E/1 + \upsilon)$ (213) = 90.3 GPa [1,4]. Eleven ψ angles, 0°, and five positive and five negative angles were evaluated. The position of the peaks was adjusted with a pseudo-Voigt function using appropriate software (WinplotR, free access online), and then converted to interplanar distances ($d\psi$) using Bragg's equation. The $d\psi$ vs. $sen2\psi$ graphs and the calculation of the slope of the linear regression (A) were done with appropriate software (Origin, Microcal, Northampton, MA, USA). The residual stress is: $\sigma = EC \times (1/d_0) \times A$; where d_0 is the interplanar distance for $\psi = 0°$ [28,29].

2.3. Corrosion Test

We prepared ten discs of as-received material (Ti6Al4V) used for machine dental implants (control group), and ten discs of Ti6Al4V cold-worked at 12.75% in order to achieve the same mechanical properties (hardness, strength, Young's modulus, strain, and residual stress) as the implantoplasty particles (experimental group). This preparation was aimed at increasing the reliability of corrosion tests. The tests with the particles included in polymeric non-conductive resin showed high deviations due to the lack of continuity of the metallic particles.

All discs were polished metallographically following the recommendations defined in ASTM E3-17 Standard [30]. Discs were treated with sequential grinding steps with different SiC papers. Samples were finally polished using diamond suspension paste with an average particle grain size ranging from 5 µm to 0.1 µm (Buehler S4, Lake Bluff, IL, USA). All metallic disc-shaped samples were smoothed up to a surface roughness (Ra) under 20 nm. Upon completion of the polishing phase, samples were cleaned with a sequential immersion bath protocol using cyclohexane, isopropanol, ethanol, deionized water, acetone, and ethanol for 15 min for each cleaning bath, together with sonication (all chemicals from Sigma Aldrich, St. Louis, MO, USA).

Testing sample groups were kept individually immersed in a constant volume of electrolyte for all the measurements. Hank's solution was selected as an electrolyte in order to simulate the real oral physiological conditions (composition displayed in Table 1). The electrolyte was kept under constant pH (6.7) during the experiments and was completely renewed for each experiment [31–33].

Table 1. Chemical composition of Hank's solution.

Chemical Composition	NaCl	KCl	Na_2HPO_4	KH_2PO_4	$CaCl_2$	$MgSO_4$	$NaHCO_3$	$C_6H_{12}0_6$
Concentration (mM)	137	5.4	0.25	0.44	1.3	1.0	4.2	5.5

The tests were carried out with a PARSTAT 2273 potentiostat (Princeton, San Jose, CA, USA) controlled by Voltamaster 4 software (Radiometer Analytical, Villeurbanne Cedex, France). For both open circuit potential measurement tests and potentiodynamic tests, the

reference electrode was a calomel electrode (saturated KCl), with a potential of 0.241 V versus the standard hydrogen electrode. The auxiliary electrode was a platinum electrode with a surface of 240 mm^2 (Radiometer Analytical, Villeurbanne, France). All the tests were carried out in a Faraday box to avoid the interaction of external electric fields. Figure 1 depicts the experimental setup of corrosion test.

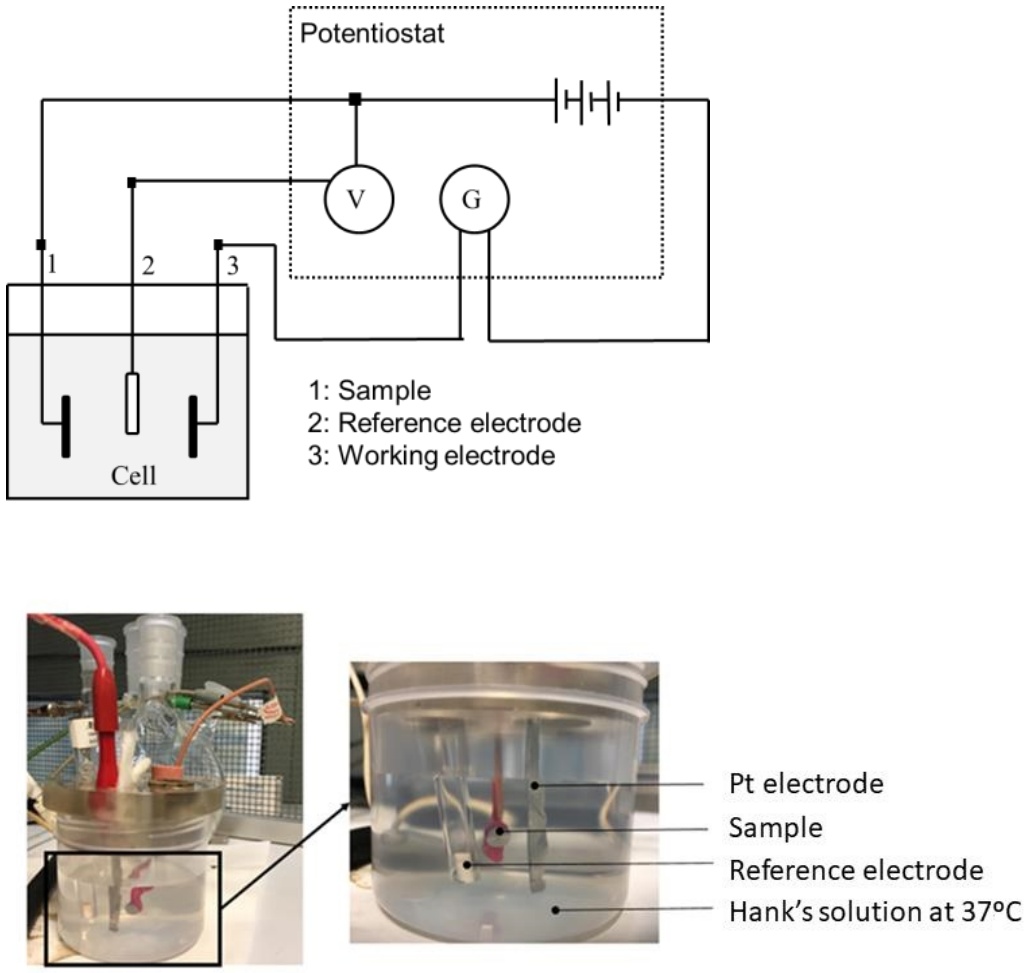

Figure 1. Three-electrode electrical circuit setup diagram and equipment used in electrochemical tests.

2.3.1. Open Circuit Potential

Tests were carried out for 5 h for all samples, taking measurements every 10 s. The potential was considered to be stabilized when the variation of the potential was less than 2 mV for a period of 30 min as indicated by the ASTM G5 and ISO 10993-5:2009 standards [31,32]. This test determines the susceptibility to corrosion (lower potential). The data and E–t curves were obtained using the PowerSuite program with the PowerCorr-Open circuit function.

2.3.2. Potentiodynamic Tests (E-$\log^{(I)}$ Curves)

Cyclic potentiodynamic polarization curves were obtained for the two study groups following the ASTM G5 standard. In this test, a potentiostat induced a variable electrical potential between the sample and the reference electrode, thus causing the passage of a current between the sample and a platinum counter electrode.

Before starting the test, the system was allowed to stabilize by means of a 5 h open-circuit test. After stabilization, a potentiodynamic test was made by means of a cyclic potential range from −0.8 mV to 1.7 mV at a rate of 2 mV/s. These parameters were

analyzed by the PowerSuite program, using the PowerCorr-Cyclic Polarization function to obtain the curves.

The parameters obtained were corrosion current density (i_{CORR} ($\mu A/cm^2$)) and corrosion potential (E_{CORR} (mV)) (value at which the current density changes from cathodic to anodic). The E_{CORR} and I_{CORR} parameters were obtained by extrapolation of the Tafel slopes [34–39].

According to ASTM G102-89, obtaining these values allows calculation of the polarization resistance (R_p) by means of the Stern–Geary expression (Equation (1)) and the corrosion rate (C_R in mm/year) (Equation (2)).

$$R_P = \frac{\beta_a \beta_c}{2.303(\beta_a + \beta_c)t_{corr}} \quad (1)$$

$$CR = K_1 \frac{t_{corr}}{\rho} EW \quad (2)$$

where $K_1 = 3.27 \times 10^{-3}$ mm-g/μA-cm-year, the density of Titanium is 4.54 g/cm^3, EW is its equivalent weight (11.98, it is considered dimensionless in these calculations), β_a is the slope of the anodic curve, and β_c the cathodic one. The polarization resistance indicates the resistance of the sample to corrosion when subjected to small variations in potential.

2.4. Statistical Analysis

Statistically significant differences were studied using statistical software (MinitabTM 13.1, Minitab Inc., State College, PA, USA). ANOVA tables with multiple comparison Fisher tests were calculated. The level of significance was established at p-value < 0.05.

3. Results

3.1. Scanning Electron Microscopy and Mechanical Properties

As described in Part I, the metal particles obtained by implantoplasty had a flattened geometry similar to "flakes" with clear signs of high levels of plastic deformation resulting from chipping (Figure 2a). The microstructure observed by SEM of the particles showed slip bands revealing the Widmanstatten plate microstructures of the Ti6Al4V alloy, which indicates that the Ti6Al4V absorbed a large deformation before the fracture. Figure 2b shows the Widmanstatten microstructure with very thin lamellar structure. The plates consisted of alpha phase plates (white phase) surrounded by beta phase plates (dark phase) [40–42].

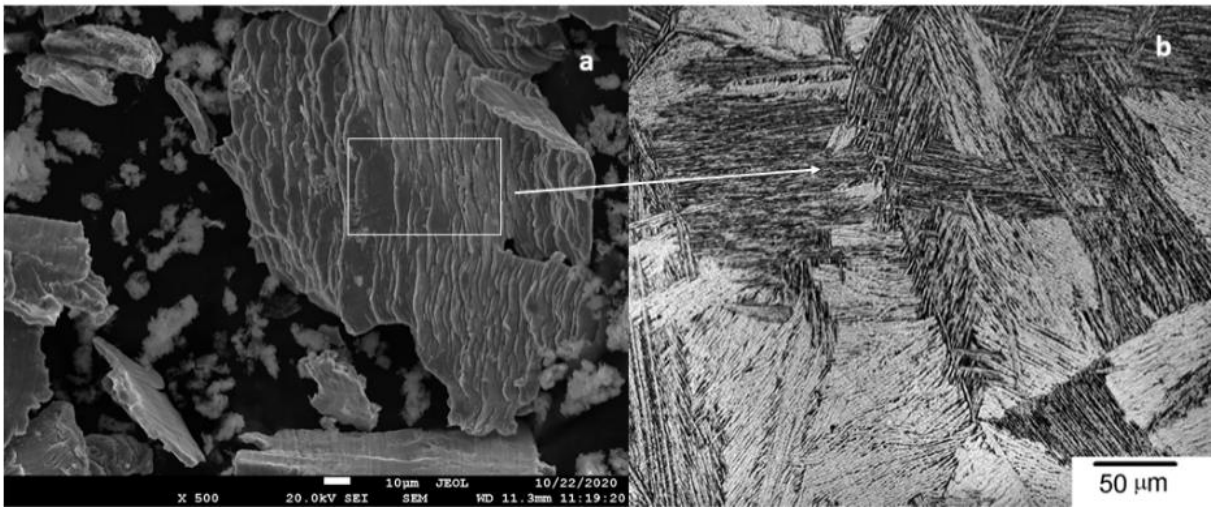

Figure 2. Scanning electron microscopy images: (**a**) implantoplasty particles at ×500 magnification; (**b**) microstructure of Widmanstatten of the particles.

Arrays of 100 indentations (10 × 10) at different loads (1, 2, 3, and 4 mN) were carried out. The hardness and elastic modulus were constant for the entire range of applied loads, as shown in Table 2. The subsequent tests (hardness and modulus of elasticity maps) were carried out at a constant load of 2 mN. At this load, the tip defect (rounding due to the manufacturing process) and the effect of polishing-induced roughness are negligible. Thus, the minimum load that allowed a correlation of mechanical properties and microstructure was selected. No statistically significant differences are obtained in the hardness and elastic modulus.

Table 2. Results of the nanoindentation test performed on dental implants.

Load, (mN)	Mean Indentation Depth (SD), (mm)	Mean Hardness (SD), (GPa)	Mean Elastic Modulus (SD), (GPa)
1	89 (3)	2.89 (0.39)	70 (5)
2	135 (5)	2.28 (0.44)	66 (4)
3	168 (5)	2.56 (0.33)	65 (3)
4	197 (5)	2.53 (0.33)	65 (3)

Abbreviations: SD = Standard deviation.

Figure 3 depicts the hardness and elastic modulus distribution maps measured on the inner and threaded surface areas of the dental implant. The comparative analysis of the results showed a joint increase in the hardness and elastic modulus of the base material (Ti6Al4V) in the threaded area as a consequence of the plastic deformation generated during the machine manufacturing processes.

The hardness and elastic modulus curves as a function of penetration depth determined for the metal debris is depicted in Figure 4.

Implantoplasty increased the hardness and elastic modulus of the metallic particles. This fact is explained because milling increased the density of dislocations and defects in the metallic structure until the implant fractured in the form of particles. As expected, the estimation of the maximum deformation decreased, as did the toughness of the metal. Residual stresses were negative in all cases, which indicates a state of compression [43,44]. Thus, the implantoplasty procedure markedly increased residual stresses.

Additionally, cold-working of 12.5% Ti6Al4V resulted in mechanical properties which are very similar to those of implantoplasty (Table 3). Thus, cold-worked disks simulate implantoplasty particles in corrosion studies. In all mechanical parameters the differences between control disks and either implantoplasty particles or cold-worked disks were significant ($p < 0.05$).

3.2. Corrosion Behavior

Open corrosion potential (E_{OCP}) is determined when a steady state is reached by the corrosion system, in which both cathodic and anodic reaction rates are properly balanced with no net current flow to or from the electrode. E_{OCP} value is used to qualitatively indicate the corrosion behavior of a material. It can be categorized as active or passive according to its sign [3,25].

Table 3. Mechanical properties obtained by nanoindentation and residual stresses determined by X-ray diffraction. The results are expressed as mean and standard deviation.

Samples	Mean Hardness (SD), (GPa)	Mean Elastic Modulus (SD), (GPa)	Max Deformation (SD), (%)	Residual Stress (SD), (MPa)
Control disks	2.2 (1.2)	65 (5)	12.0 (4.2)	−27.5 (5.2)
Implantoplasty	4.8 (1.0)	80 (9)	4.3 (0.7)	−354.5 (35.2)
Ti cold-worked disks	4.7 (0.9)	78 (8)	4.0 (0.5)	−345 (3.2)

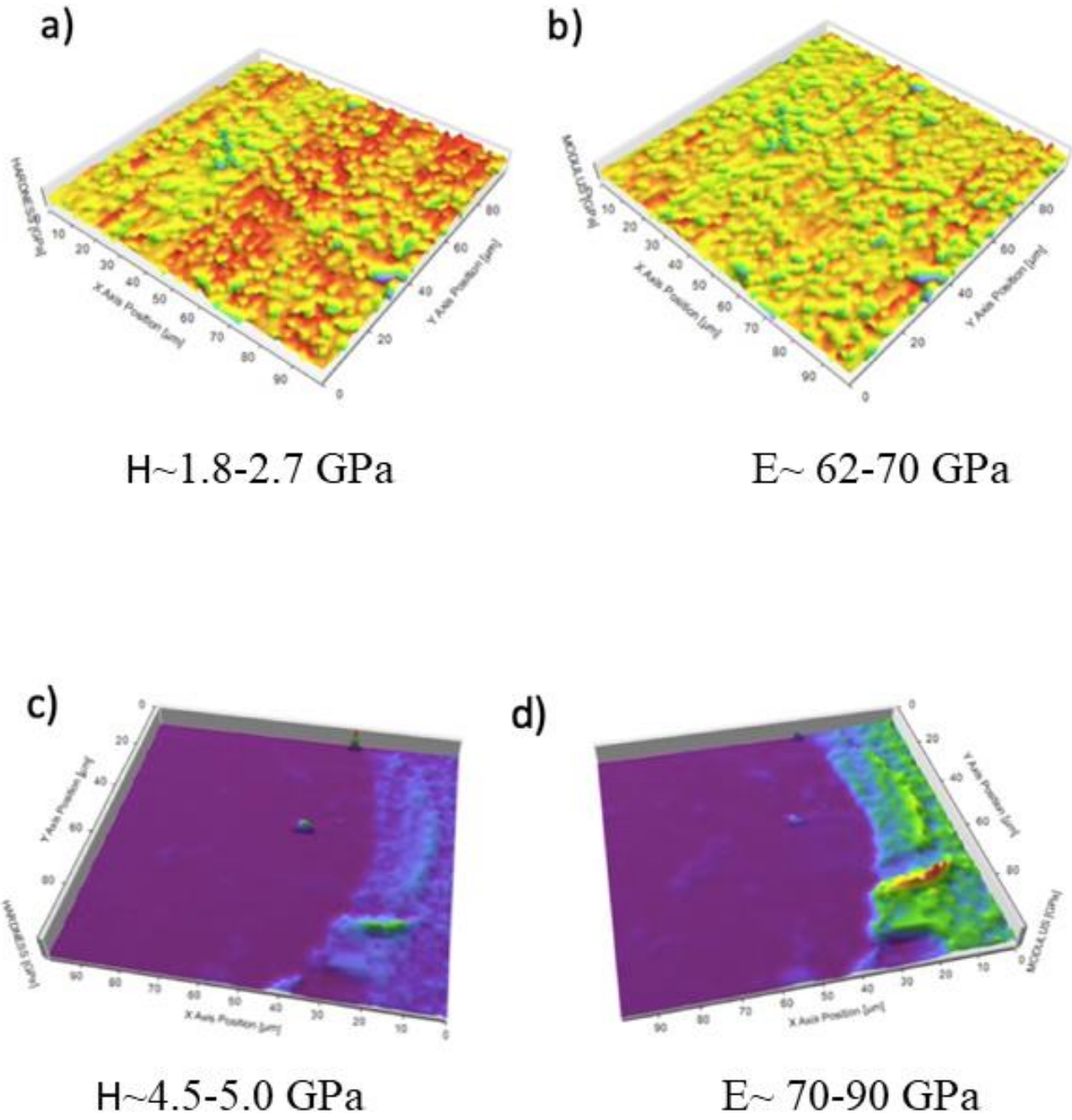

Figure 3. (**a**) Map of hardness distribution of the inner zone of the screw; (**b**) map of elastic modulus of the inner zone of the screw; (**c**) map of hardness of the surface zone of the screw; (**d**) map of elastic modulus of the surface of the screw. Figure 3 shows the hardness and elastic modulus curves as a function of penetration depth determined for the metal debris. Particles were harder than the base material. On the other hand, the elastic modulus of the metal debris showed values similar to those of the implant thread area.

The open circuit potential (E_{OCP}) results are shown in Figure 5. The potential was on average -204 ± 18 mV for the titanium control, and -254 ± 3 mV ($p < 0.05$) for the implantoplasty samples, which means that the titanium control was more electropositive and in consequence more resistant to corrosion.

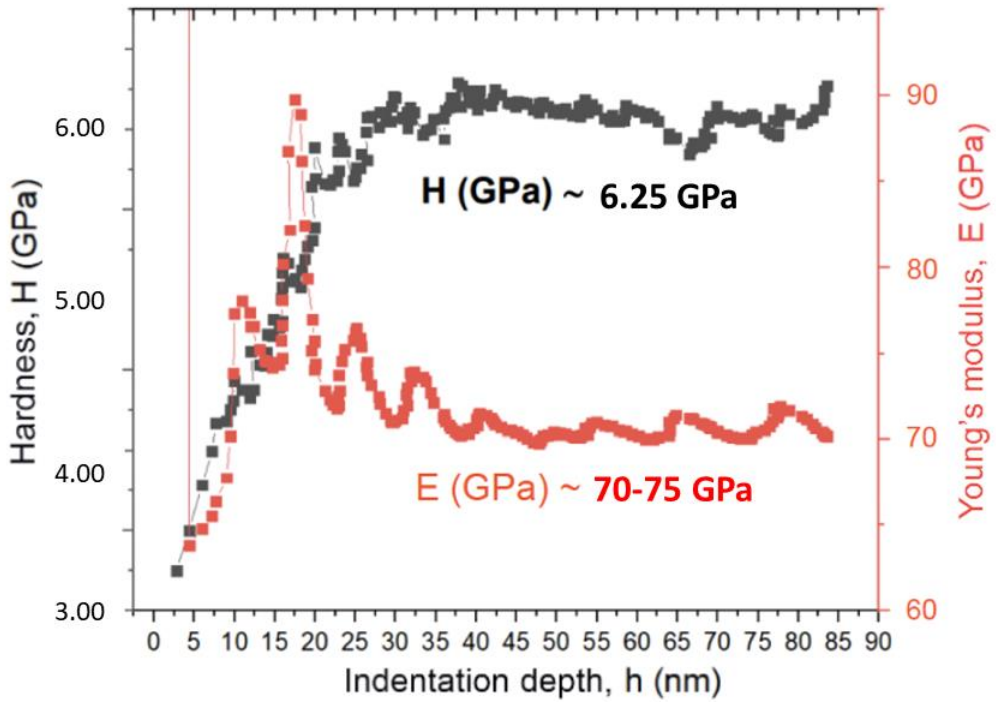

Figure 4. Hardness and elastic modulus curves according to indentation depth of the particles of the metal debris.

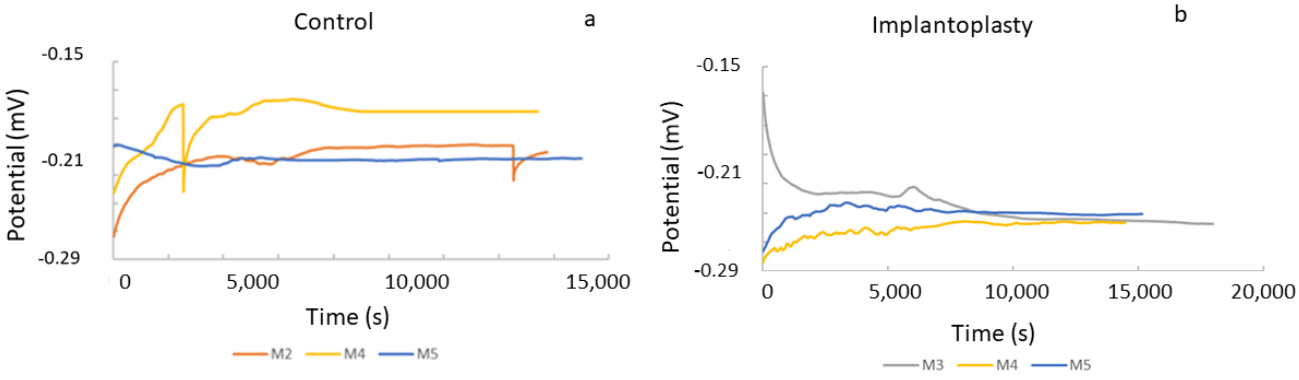

Figure 5. Curves of the open circuit potential for (**a**) control disc (original dental implant material) and (**b**) implantoplasty samples.

The potentiodynamic curves of the two groups can be observed in Figure 6. For all the calculated parameters, the control group presents better corrosion resistance than the implantoplasty group, since its E_{CORR}, I_{CORR}, and corrosion rate values are lower, and the polarization resistance is higher (Table 4). However, these differences were not statistically significant for any of the mentioned parameters ($0.15 > p > 0.05$).

Table 4. Electrochemical parameters obtained by the potentiodynamic curves for control and implantoplasty samples. The results are expressed as mean ± standard deviation.

Samples	Ecorr (SD), (mV)	Icorr (SD), ($\mu A/cm^2$)	Polarization Resistance (SD), (Ω/cm^2)	Corrosion Rate (SD), (mm/Year)
Control disks	−340 (32)	0.051 (0.007)	1.14×10^6 (1.13×10^5)	4.44×10^{-4} (6.69×10^{-5})
Implantoplasty	−368 (47)	0.055 (0.005)	1.07×10^6 (1.77×10^5)	4.77×10^{-4} (4.46×10^{-5})

Figure 7 depicts SEM images of the surfaces of the control and implantoplasty samples after the corrosion tests. We selected areas with machining failures, as they are the most susceptible to corrosion. The implantoplasty sample showed much pitting, while the control sample did not display any [45].

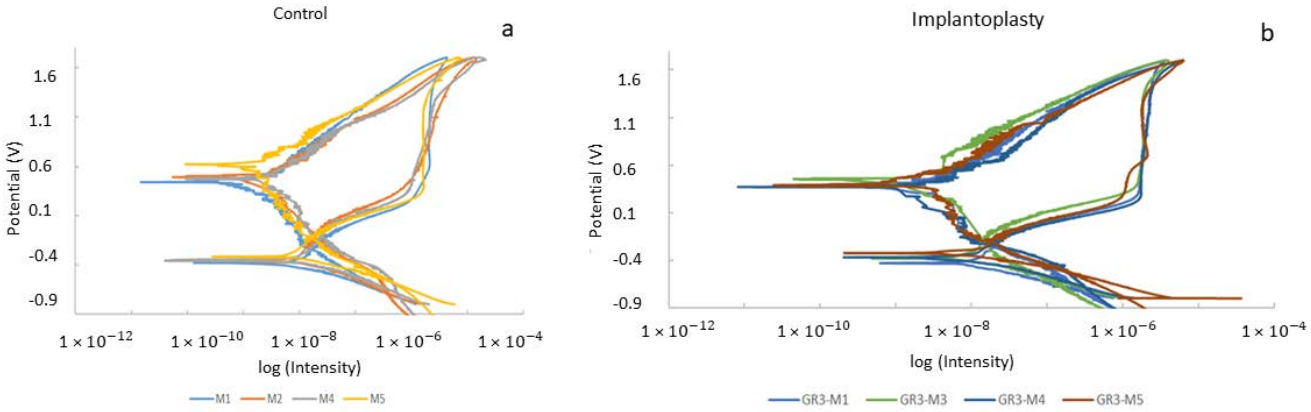

Figure 6. Potentiodynamic curves for (**a**) control disc (original dental implant material) and (**b**) implantoplasty samples.

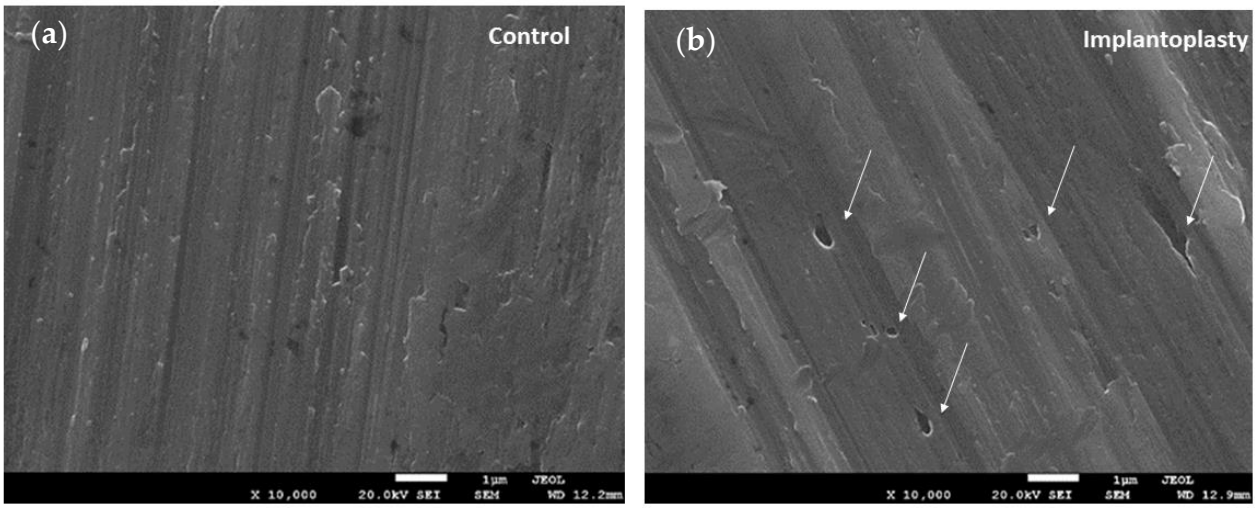

Figure 7. SEM images of the surfaces for (**a**) control and (**b**) implantoplasty samples.

4. Discussion

Nanoindentation tests showed that the Ti alloy particles released during implantoplasty were harder, probably because of the stress applied during machining. It is well known that when metals are machined, defects in the crystalline lattice (band slips, twins, etc.) increase the hardness of the metal to the point that it cannot absorb any more energy, causing it to fracture at those points. Thus, these particles have much higher internal energy than the rest of the dental implant. According to the laws of thermodynamics, the system will release energy to become more stable, thus being more susceptible to ion release and electrochemical corrosion; this can therefore generate non-cytocompatible oxides [3,46]. Although there is no joint wear in the oral cavity, implantoplasty milling procedures could have a similar effect, though not sustained over time. Moreover, in the oral cavity, the presence of physiological fluids and the stable temperature of 37 °C favor this release of ions and corrosion of the metal [28,47]. Therefore, from our point of view, the main risk of implantoplasty lies in the high internal energy of the metal debris produced, since its reaction with the medium to lower the internal energy levels may give rise to products or interactions that exert a toxic effect upon the physiological environment, especially human

cells. Thus, implantoplasty might imply a risk of contributing to implant failure over the medium to long term, due to aseptic bone loss. In addition, there is also the risk of an increased presence of metal ions in the blood and their accumulation in the organs.

As Figure 6 shows, there was an almost constant open corrosion potential over immersion time in all samples. This signal (potential) stability would be directly connected to the formation of a stable Ti-oxide passive film. The stability of this inert film depends to a great extent on the volume of the newly formed oxides. In the case of Ti6Al4V, there are several mixed oxides (non-stoichiometric oxides), which should be as similar as possible to the volume of the base-metal in order to protect the metal against corrosion. This happens particularly in the case of Ti6Al4V for all the oxides, which usually leads to the formation of thin passive films with oxide volumes very similar to the bulk metals, thus avoiding the formation of both cracks and breaks. This favors the passivity of the Ti6Al4V alloys.

The corrosion potential results showed that control samples had the best corrosion resistance. As-received material presented a good chemical homogeneity as a result of an annealing treatment. In addition, annealing heat treatment avoided the presence of residual stresses, which could favor the decrease of galvanic corrosion rates. Implantoplasty samples showed a decrease in the corrosion potential due to the residual stress induced by the machining process on the surface [48–52], which can enhance surface chemical reactivity during corrosion testing. As is well-known, machining of metals induces residual stresses, which can affect their in-service behavior, as reported by several authors [53,54]. Corrosion resistance can be decreased by the presence of other metallic elements in the mouth (stainless steel wires for orthodontics, metals for prosthetics, among others) that create a galvanic current due to the presence of metallic materials of different chemical natures in an electrochemical environment.

Finally, SEM shows the presence of pitting on the implantoplasty surfaces due to the electrochemical corrosion. Pitting involves a loss of material due to corrosion by migration of the reaction product (titanium oxide) into the physiological medium. These particles released as a result of corrosion and/or mechanical treatment, such as implantoplasty, have been reported to cause adverse allergic reactions in humans [55,56]. There is no current consensus on the risk of particles released from titanium implants; however, it would be prudent for clinicians to carefully evaluate the materials used, and to consider the potential risks of the individual constituents of any alloy, as indicated in this study.

5. Conclusions

Ti6Al4V alloy particles released during implantoplasty show higher hardness, mechanical strength, and compressive residual stresses than the control Ti6Al4V material. These compressive residual stresses, due to the higher deformation in the Widmanstatten microstructure, cause inferior corrosion behavior, both in open circuit potential and in potentiodynamic tests. Implantoplasty particles present worse corrosion resistances than the original samples, since their E_{CORR}, I_{CORR}, and corrosion rate values are higher, and the polarization resistance is lower. The increase in corrosion rate due to implantoplasty causes pitting on the surface of the samples. Clinicians must be aware of the potential risks of implantoplasty, because of a reduction in corrosion resistance among metal particles released during this procedure.

Author Contributions: Conceptualization: M.Á.S.-G., C.G.-E., E.V.-C., O.C.-F. and F.J.G.; methodology: M.Á.S.-G., C.G.-E., E.V.-C., O.C.-F. and F.J.G.; software: J.T.-S., M.M. and P.V.; validation: J.T.-S., M.M., P.V. and E.V.-C..; formal analysis: M.Á.S.-G., C.G.-E., E.V.-C., O.C.-F. and F.J.G.; investigation, J.T.-S., P.V. and M.M.; resources, E.V.-C. and M.Á.S.-G.; data curation, O.C.-F., C.G.-E., E.V.-C. and J.T.-S.; writing—original draft preparation: J.T.-S., P.V. and F.J.G.; writing—review and editing, M.Á.S.-G., C.G.-E., E.V.-C. and O.C.-F.; visualization: E.V.-C.; supervision: M.Á.S.-G., C.G.-E., E.V.-C., O.C.-F. and F.J.G.; project administration: E.V.-C.; funding acquisition: E.V.-C. All authors have read and agreed to the published version of the manuscript.

Funding: This study was supported by the *Instituto de Salud Carlos III* through project PI20/01596 (co-funded by the European Regional Development Fund (ERDF), a way to build Europe). In addition, this research received funding from the Spanish government for financial support through the projects, RTI2018-098075-B-C21, and RTI2018-098075-BC22, co-funded by the EU through the European Regional Development Funds (MINECO-FEDER, EU).

Institutional Review Board Statement: Not applicable.

Informed Consent Statement: Not applicable.

Acknowledgments: We thank CERCA Programme/Generalitat de Catalunya for institutional support, Dental implants were kindly provided by the Avinent Implant System, Santpedor, Spain.

Conflicts of Interest: Jorge Toledano-Serrabona has received no grants, personal fees, or non-financial support. Octavi Camps-Font has participated as co-investigator in clinical trials sponsored by Mundipharma (Cambridge, UK) and Menarini Richerche (Florence, Italy). He also reports grants and non-financial support from Avinent (Santpedor, Spain). Eduard Valmaseda-Castellón reports personal fees and non-financial support from MozoGrau (Valladolid, Spain). He is the Director of the Avinent—University of Barcelona research agreement (Càtedra UB–Avinent), with Avinent (Santpedor, Spain), and has received personal fees from BioHorizons Ibérica (Madrid, Spain), Inibsa Dental (Lliça de Vall, Spain), and Dentsply implants Iberia (Barcelona, Spain) outside the submitted work. In addition, Valmaseda-Castellón has participated as an investigator in clinical trials sponsored by Mundipharma (Cambridge, UK) and Geistlich (Wolhusen, Switzerland). Cosme Gay-Escoda reports grants, personal fees, and non-financial support from Mundipharma (Cambridge, UK) and Menarini Richerche (Florence, Italy). María Ángeles Sánchez-Garcés reports grants, personal fees, and non-financial support from Nobel Biocare, Zimmer, and Menarini Richerche (Florence, Italy). Pablo Verdeguer has received no grants, personal fees, or non-financial support. Mertixell Molmeneu has received no grants, personal fees, or non-financial support. F. Javier Gil reports grants from the Spanish government, European Union personal fees, and non-financial support from Klockner Dental Implants (Barcelona, Spain).

References

1. Alrabiah, M.; Alrahlah, A.; Al-Hamdan, R.S.; Al-Aali, K.A.; Labban, N.; Abduljabbar, T. Survival of adjacent-dental-implants in prediabetic and systemically healthy subjects at 5-years follow-up. *Clin. Implant Dent. Relat. Res.* **2019**, *21*, 232–237. [CrossRef]
2. Francetti, L.; Cavalli, N.; Taschieri, S.; Corbella, S. Ten years follow-up retrospective study on implant survival rates and prevalence of peri-implantitis in implant-supported full-arch rehabilitations. *Clin. Oral Implant. Res.* **2019**, *30*, 252–260. [CrossRef]
3. Aparicio, C.; Gil, F.J.; Fonseca, C.; Barbosa, M.; Planell, J.A. Corrosion behaviour of commercially pure titanium shot blasted with different materials and sizes of shot blasted with different materials and sizes of shot particles for dental implant applications. *Biomaterials* **2003**, *24*, 263–273. [CrossRef]
4. Ratner, B.D. A Perspective on Titanium Biocompatibility. In *Titanium in Medicine: Material Science, Surface Science, Engineering, Biological Responses and Medical Applications*; Brunette, D.M., Tengvall, P., Textor, M., Thomsen, P., Eds.; Springer: Berlin, Germany, 2001; pp. 1–12.
5. Aparicio, C.; Rodríguez, D.; Gil, F.J. Variation of roughness and adhesion strength of deposited apatite layers on titanium dental implants. *Mat. Sci. Eng. C* **2011**, *31*, 320–324. [CrossRef]
6. Zhang, L.C.; Chen, L.Y. A review on biomedical titanium alloys: Recent progress and prospect. *Adv. Eng. Mater.* **2019**, *21*, 1801215. [CrossRef]
7. Dias Corpa Tardelli, J.; Bolfarini, C.; Cândido Dos Reis, A. Comparative analysis of corrosion resistance between beta titanium and Ti6Al4V alloys: A systematic review. *J. Trace Elem. Med. Biol.* **2020**, *62*, 126618. [CrossRef]
8. Berbel, L.O.; Banczek, E.; Karoussis, I.K.; Kotsakis, G.A.; Costa, I. Determinants of corrosion resistance of Ti6Al4V alloy dental implants in an In Vitro model of peri-implant inflammation. *PLoS ONE* **2019**, *14*, e0210530.
9. Gai, X.; Bai, Y.; Li, S.; Hou, W.; Hao, Y.; Zhang, X.; Yang, R.; Misra, R. In-situ monitoring of the electrochemical behavior of cellular structured biomedical Ti6Al4V alloy fabricated by electron beam melting in simulated physiological fluid. *Acta Biomater* **2020**, *106*, 387–395. [CrossRef]
10. Willis, J.; Li, S.; Crean, S.J.; Barrak, F.N. Is titanium alloy Ti-6Al-4 V cytotoxic to gingival fibroblasts—A systematic review. *Clin. Exp. Dent. Res.* **2021**. [CrossRef]
11. Challa, V.S.; Mali, S.; Misra, R.D. Reduced toxicity and superior cellular response of preosteoblasts to Ti-6Al-7Nb alloy and comparison with Ti6Al4V. *J. Biomed. Mater. Res. A* **2013**, *101*, 2083–2089. [CrossRef] [PubMed]
12. Schwarz, F.; Derks, J.; Monje, A.; Wang, H.L. Peri-implantitis. *J. Clin. Periodontol.* **2018**, *45*, 246–266. [CrossRef] [PubMed]
13. Figuero, E.; Graziani, F.; Sanz, I.; Herrera, D.; Sanz, M. Management of peri-implant mucositis and peri-implantitis. *Periodontology* **2014**, *66*, 255–273. [CrossRef] [PubMed]

14. Batalha, V.C.; Bueno, R.A.; Fronchetti Junior, E.; Mariano, J.R.; Santin, G.C.; Freitas, K.M.S.; Ortiz, M.A.L.; Salmeron, S. Dental implants surface in vitro decontamination protocols. *Eur. J. Dent.* **2021**, *15*, 407–411. [CrossRef] [PubMed]
15. Buser, D. Titanium for dental applications (I). In *Titanium in Medicine: Material Science, Surface Science, Engineering, Biological Responses and Medical Applications*; Brunette, D.M., Tengvall, P., Textor, M., Thomsen, P., Eds.; Springer: Berlin, Germany, 2001; pp. 875–888.
16. Thomsen, P.; Larsson, C.; Ericsson, L.E.; Sennerby, L.; Lausmaa, J.; Kasemo, B. Bone response to machined cast titanium implants. *J. Mater. Sci. Mater. Med.* **1997**, *8*, 653–665. [CrossRef]
17. Pegueroles, M.; Tonda-Turo, C.; Planell, J.A.; Gil, F.J.; Aparicio, C. Adsorption of fibronectin, fibrinongen, and albumin on TiO_2: Time-resolved kinetics, structural changes, and competition study. *Biointerphases* **2012**, *7*, 48–61. [CrossRef] [PubMed]
18. Guillem, J.; Delgado, L.; Godoy-Gallardo, M.; Pegueroles, M.; Herrero, M.; Gil, F.J. Fibroblast adhesion and activation onto micro-machined titanium surfaces. *Clin. Oral Implant. Res.* **2013**, *24*, 770–780. [CrossRef]
19. Pegueroles, M.; Aparicio, C.; Bosio, M.; Engel, E.; Gil, F.J.; Planell, J.A.; Altankov, G. Spatial organization of osteoblast fibronectin-matrix on titanium surface—Effects of roughness, chemical heterogeneity, and surface free energy. *Acta Biomater.* **2010**, *6*, 291–301. [CrossRef]
20. Williams, D.F. Titanium for medical applications. In *Titanium in Medicine: Material Science, Surface Science, Engineering, Biological Responses and Medical Applications*; Brunette, D.M., Tengvall, P., Textor, M., Thomsen, P., Eds.; Springer: Berlin, Germany, 2001; pp. 13–24.
21. Schliephake, H.; Scharnweber, D. Chemical and biological functionalization of titanium for dental implants. *J. Mater. Chem.* **2008**, *18*, 2404–2414. [CrossRef]
22. Brunski, J.B. Classes of materials used in medicine. Metals. In *Biomaterials Science, an Introduction to Materials in Medicine*; Rutner, B., Hoffman, A., Schoen, F., Lemons, J., Eds.; Academic Press: San Diego, CA, USA, 1996; pp. 137–152.
23. Velasco-Ortega, E.; Jiménez-Guerra, A.; Monsalve-Guil, L.; Ortiz-García, I.; Nicolás-Silvente, A.I.; Segura-Egea, J.J.; Lopez-Lopez, J. Long-term clinical outcomes of treatment with dental implants with acid etched surface. *Materials* **2020**, *13*, 1553. [CrossRef]
24. Manero, J.M.; Gil, F.J.; Padrós, A.; Planell, J.A. Applications of environmental scanning electron microscopy (ESEM) in biomaterials field. *Microsc. Res. Tech.* **2003**, *61*, 469–480. [CrossRef]
25. Delgado-Ruiz, R.; Romanos, G. Potential causes of titanium particle and ion release in implant dentistry: A systematic review. *Int. J. Mol. Sci.* **2018**, *19*, 3585. [CrossRef]
26. Costa-Berenguer, X.; García-García, M.; Sánchez-Torres, A.; Sanz-Alonso, M.; Figueiredo, R.; Valmaseda-Castellón, E. Effect of implantoplasty on fracture resistance and surface roughness of standard diameter dental implants. *Clin. Oral Implant. Res.* **2018**, *29*, 46–54. [CrossRef]
27. Camps-Font, O.; González-Barnadas, A.; Mir-Mari, J.; Figueiredo, R.; Gay-Escoda, C.; Valmaseda-Castellón, E. Fracture resistance after implantoplasty in three implant-abutment connection designs. *Med. Oral Patol. Oral Cir. Bucal* **2020**, *25*, 691–699. [CrossRef]
28. Velasco, E.; Monsalve-Guil, L.; Jimenez, A.; Ortiz, I.; Moreno-Muñoz, J.; Nuñez-Marquez, E.; Pegueroles, M.; Pérez, R.A.; Gil, F.J. Importance of the roughness and residual stresses of dental implants on fatigue and osseointegration behavior. In vivo study in rabbits. *J. Oral Implantol.* **2016**, *42*, 469–476. [CrossRef]
29. Pérez, R.A.; Gargallo, J.; Altuna, P.; Herrero-Climent, M.; Gil, F.J. Fatigue of narrow dental implants: Influence of the hardening method. *Materials* **2020**, *13*, 1429. [CrossRef]
30. ASTM-E3-11. *Standard Guide for Preparation of Metallographic Specimens*; ASTM International: West Conshohocken, PA, USA, 2017.
31. *Standard Reference Test Method for Making Potentiostatic and Potentiodynamic Anodic Polarization Measurements*; Technical Report no. ASTM G5-14e1; ASTM International: West Conshohocken, PA, USA, 2014.
32. ISO 10993-5:2009. Part 5: Tests for In Vitro Cytotoxicity. In *Biological Evaluation of Medical Devices*; International Organization for Standardization: Geneve, Switzerland, 2009.
33. Mansfeld, F.; Kenkel, J.V. Laboratory studies of galvanic corrosion of aluminium alloys. In *Galvanic and Pitting Corrosion-Field and Laboratory Studies*; Baboian, R., France, W., Roew, L., Rynewicz, J., Eds.; ASTM: Philadelphia, PA, USA, 1976; pp. 20–47.
34. Mansfeld, F. The polarization resistance technique for measuring corrosion currents. In *Advances in Corrosion Science and Technology*; Fontana, M.G., Staehle, R.W., Eds.; Springer: Boston, MA, USA, 1976; pp. 89–92.
35. Canay, S.; Öktemer, M. In vitro corrosion behaviour of 13 prosthodontic alloys. *Quintessence Int.* **1992**, *23*, 279–287.
36. Senna, P.; Antoninha Del Bel Cury, A.; Kates, S.; Meirelles, L. Surface damage on dental implants with release of loose particles after insertion into bone. *Clin. Implant. Dent. Relat. Res.* **2015**, *17*, 681–692. [CrossRef]
37. Barbieri, M.; Mencio, F.; Papi, P.; Rosella, D.; Di Carlo, S.; Valente, T.; Pompa, G. Corrosion behavior of dental implants immersed into human saliva: Preliminary results of an in vitro study. *Eur. Rev. Med. Pharmacol. Sci.* **2017**, *21*, 3543–3548.
38. Boyer, R.; Welsch, G.; Collings, W. *Materials Properties Handbook: Titanium Alloys*; ASM International: Novelty, OH, USA, 1994.
39. Reclaru, L.; Meyer, J.M. Study of corrosion between a titanium implant and dental alloys. *J. Dent.* **1994**, *22*, 159–168. [CrossRef]
40. Ginebra, M.P.; Gil, F.J.; Manero, J.M.; Planell, J.A. Formation of α- Widmanstatten structure: Effects of grain size and cooling rate on the Widmanstatten morphologies and on the mechanical properties in Ti6Al4V alloy. *J. Alloys Compd.* **2001**, *329*, 142–152.
41. Gil, F.J.; Manero, J.M.; Ginebra, M.P.; Planell, J.A. The effect of cooling rate on the cyclic deformation of β-annealed Ti6Al4V. *Mat. Sci. Eng.* **2003**, *349*, 150–155. [CrossRef]
42. Manero, J.M.; Gil, F.J.; Planell, J.A. Deformation mechanisms of Ti6Al4V alloy with a martensitic microstructure subjected to oligocyclic fatigue. *Acta Mater.* **2000**, *48*, 3353–3359. [CrossRef]

43. Gil, F.J.; Planell, J.A.; Padrós, A.; Planell, J.A. Fracture and fatigue behaviour of shot blasted titanium dental implants. *Impl. Dent.* **2002**, *11*, 28–32. [CrossRef] [PubMed]
44. Porter, D.A.; Easterling, K.E.; Sheriff, M. *Phase Transformation in Metals and Alloys*, 3rd ed.; CRC Press: Boca Raton, FL, USA, 2013.
45. Geis-Gerstorfer, J. In vitro corrosion measurements of dental alloys. *J. Dent.* **1994**, *22*, 247–251. [CrossRef]
46. Gil, F.J.; Planell, J.A.; Padrós, A.; Aparicio, C. The effect of shot blasting and heat treatment on the fatigue behavior of titanium for dental implant applications. *Dent. Mater.* **2007**, *23*, 486–491. [CrossRef]
47. Gil, F.J.; Espinar, E.; Llamas, J.M.; Sevilla, P. Fatigue life of bioactive titanium dental implants treated by means of grit-blasting and thermo-chemical treatment. *Clin. Implant. Dent. Relat. Res.* **2014**, *16*, 273–281. [CrossRef]
48. Wataha, J.C.; Lockwood, P.E.; Khajotia, S.S. Effect of pH on element release from dental casting alloys. *J. Prosthet. Dent.* **1998**, *80*, 691–698. [CrossRef]
49. Gil, F.J.; Rodríguez, D.; Planell, J.A.; Cortada, M.; Giner, L.; Costa, S. Galvanic corrosion behaviour of Titanium implants coupled to dental alloys. *J. Mat. Sci. Mat. Med.* **2000**, *11*, 287–293. [CrossRef]
50. Brånemark, P.I.; Hansson, I.; Adell, R.; Lindstrom, U.; Hallen, J.; Ohman, O. Osseointegrated implants in the treatment of the edentulous jaw. Experience from a 10-year period. *Scand. J. Plast. Reconstr. Surg. Suppl.* **1977**, *16*, 1–132. [PubMed]
51. Adell, R.; Lekholm, U.; Rocker, U.; Brånemark, P.I. A 15-year study of osseointegrated implants in the treatment of the treatment of the edentulous jaw. *Int. J. Oral Surg.* **1981**, *6*, 387–416. [CrossRef]
52. Sarkar, N.K.; Fuys, R.A.; Stanford, J.W. Applications of electrochemical techniques to characterize the corrosion of dental alloys. In *Corrosion and Degradation of Implant Materials*; Syrett, B.C., Acharya, A., Eds.; ASTM: Philadelphia, PA, USA, 1979; pp. 277–294.
53. Hosoki, M.; Bando, E.; Asaoka, K.; Takeuchi, H.; Nishigawa, K. Assessment of allergic hypersensivity to dental materials. *Biomed. Mater. Eng.* **2009**, *19*, 53–61. [CrossRef] [PubMed]
54. Mombelli, A.; Hashim, D.; Cionca, N. What is the impact of titanium particles and bioocorrosion on implant survival and complications? A critical review. *Clin. Oral Implant. Res.* **2018**, *29*, 37–53. [CrossRef]
55. Harloff, T.; Hönle, W.; Holzwarth, U.; Bader, R.; Yhomas, P.; Schuh, A. Titanium allergy or not? "Impurity" of titanium implant materials. *Health* **2010**, *2*, 306–310. [CrossRef]
56. Chaturvedi, T. Allergy related to dental implant and its clinical significance. *Clin. Cosmet. Investig. Dent.* **2013**, *5*, 57–61. [CrossRef] [PubMed]